

## Regular article

# Theoretical analysis of some substituted imine–enamine tautomerism

Patricia Pérez, Alejandro Toro-Labbé

Departamento de Química Física, Facultad de Química, Pontificia Universidad Católica de Chile, Casilla 306, Correo 22, Santiago, Chile

Received: 21 August 2000 / Accepted: 14 September 2000 / Published online: 19 January 2001  
© Springer-Verlag 2001

**Abstract.** We present a theoretical study of the  $\text{CH}_3\text{CXNH} \rightleftharpoons \text{CH}_2\text{CXNH}_2$  tautomerism. The analysis is performed in terms of global descriptors of reactivity, such as electronic chemical potential, chemical hardness and chemical softness. Chemical hardness is used to study the relative stability in the frame of the maximum hardness principle. Chemical softness appears to be related to the molecular polarizability, and it is used to discuss relative stability in the context of the minimum polarizability principle. Both empirical rules are simultaneously satisfied for this equilibrium. Transition states, in which the transferred proton is found about midway between the donor and acceptor atoms, are rationalized in terms of the Brønsted coefficient for the relative position along the reaction coordinate and the Marcus equation for the energy barriers. Substituent effects on the activation properties are analyzed in a partitioned form that probes the effect of the substituent group on the molecular properties at the ground-state and transition-state structures.

**Key words:** Imine–enamine tautomerism – Hardness profile – Polarizability profile – Proton transfer – Transition state

## 1 Introduction

It is well known that tautomerism is one of the fundamental processes in organic chemistry. It has been extensively studied [1–6] and it is still receiving renewed interest because of the improved experimental and theoretical methods. These equilibria also have a recognized importance in biological processes. Among these rearrangements, the most investigated and documented are the keto  $\rightleftharpoons$  enol equilibria [7–12]; however,

fewer studies have been done on the imine  $\rightleftharpoons$  enamine equilibria. Methanimine ( $\text{CH}_2=\text{NH}$ ), the simplest imine, was first predicted by Leermaker [13] in 1933. It was proposed as an intermediate in the pyrolysis of methyl azide by Rice and Grelecki [14]. Methanimine was observed in a mass spectrometer by Collin and Franks in 1966 [15]. In 1972 Johnson and Lovas [16] determined the structure of  $\text{CH}_2=\text{NH}$  by microwave spectroscopy. The experimental geometry was in good agreement with that predicted from theoretical calculations [17, 18]. In 1980 Lovas et al. [19] separated and determined the structures of cis and trans acetaldimines in a microwave spectrometer. Theoretical studies on vinylamine ( $\text{CH}_2\text{CHNH}_2$ ) and acetaldimine ( $\text{CH}_3\text{CHNH}$ ) were conducted by Pross, Radom and Riggs [20]. These authors reported the relative stabilities of the different conformers of acetaldimine. Recently, Lammertsma and Prasad [21] reported a G2 study on the thermodynamics of the tautomeric pair acetaldimine  $\rightleftharpoons$  vinylamine.

In the absence of experimental data, it is of special interest to characterize theoretically the imine  $\rightleftharpoons$  enamine tautomeric equilibria to obtain information about the thermodynamic and kinetic aspects. Recently, Lin et al. [22] have reported an ab initio study on the  $\alpha$ -substituted acetaldimines  $\text{XH}_2\text{CCH}=\text{NH}$  to investigate the substituent effects on the imine  $\rightleftharpoons$  enamine equilibria. These authors found that enamines were favored over the imines owing to the conjugative interaction between the  $\text{C}=\text{C}$  double bonds and the empty  $p$  orbital in boron ( $X = \text{BH}_2$ ) and the interaction of the  $\text{C}=\text{C}$  bond with the  $\pi^*$  orbitals when  $X = \text{NO}$  and  $X = \text{CN}$ .

In the recent years, density functional theory (DFT) [23, 24] has been shown to be a versatile tool in many branches of physics and chemistry [25]. In electronic structure theory, it has not only generated useful schemes for computation but it has also provided a framework to introduce new concepts [23, 24]. Among others, one finds the concepts of electronic chemical potential ( $\mu$ ) [26], chemical hardness ( $\eta$ ) [27], chemical softness [28], local softness [29], the Fukui function [30], etc. Even though these concepts had been introduced earlier, only in recent years have they received stronger

Correspondence to: A. Toro-Labbé  
e-mail: atola@puc.cl

attention. Many authors are using these concepts to rationalize and to understand chemical reactions [31]. The study of energy, electronic chemical potential, and molecular hardness profiles has been shown to be useful to rationalize the relative stability and reactivity of different species on the potential-energy surface [32–35]. These quantities are better appreciated when they are used in connection with empirical rules of reactivity, such as the maximum hardness principle (MHP), the hard and soft acids and bases (HSAB) principle and the minimum polarizability principle (MPP). The MHP states that “there seems to be a rule of nature that molecules arrange themselves so as to be as hard as possible” [24, 36, 37], so that molecular systems at equilibrium tend to states of highest hardness. The transition states (TSs) are expected to present a minimum value of  $\eta$ . This empirical rule permits the establishment of a bridge connecting electronic and energetic properties. The HSAB principle establishes that “hard acids prefer to coordinate to hard bases, and soft acids prefer to coordinate to soft bases” [24, 27, 38]. On the basis of an inverse relationship between  $\alpha$  and  $\eta$  [39], Chattaraj and Sengupta [40] have proposed the MPP, which states that “the natural direction of evolution of any system is toward a state of minimum polarizability”. It has also been shown that “a system is harder and less polarizable in its ground state than in any of its excited states” [41]. The polarizability ( $\alpha$ ) of the system may be used to understand the behavior of the system for changing the external potential,  $v(\vec{r})$ , at a constant number of electrons,  $N$  [42].

The electronic descriptors of reactivity together with the empirical rules are useful objects to understand and justify other classical empirical model of reactivity, such as the Hammond postulate [43]. The Hammond postulate permits insights into the structure and properties of the TSs from the knowledge of the structure and properties of reactants and products [34, 44]; it is an important concept in chemistry basically because it provides a connection between the kinetics and thermodynamics of chemical reactions.

In this work, we present a theoretical study on the tautomeric equilibria  $\text{CH}_3\text{CX}=\text{NH} \rightleftharpoons \text{CH}_2=\text{CXNH}_2$  with  $X = \text{H, F, Cl, Br, NH}_2, \text{CH}_3, \text{OH}$  and  $\text{N}(\text{CH}_3)_2$ . Global properties such as  $\mu$ ,  $\eta$  and  $\alpha$  are used to describe the different aspects of this interconversion, including energy barriers and the substituent effects in the relative stability of the isomers. These electronic indices will be used in connection with the empirical principles of chemical reactivity to rationalize the relative stability of the molecules.

## 2 Theoretical background

### 2.1 General definitions

The imine  $\rightleftharpoons$  enamine equilibria will be represented by three stationary points R, TS and P, where R represents the ground state of the imine form (reactant), TS represents the transition state structure and P the corresponding ground state of the enamine (product).

We introduce a reduced reaction coordinate,  $\omega$ , to connect R and P. This coordinate  $\omega$ , measures the reaction progress in going from reactants ( $\omega = 0$ ) to products ( $\omega = 1$ ) [33–35]. It can be defined through a scaling procedure on the internal reaction coordinate (IRC) obtained from ab initio calculations, an IRC calculation gives the reaction path leading down to reactants and products from the TS.

Formal definitions of  $\eta$  and  $\mu$  have been given by Parr and coworkers and Pearson [23, 24, 36, 37]. A three-point finite difference approximation leads to the following working formulae of these quantities:

$$\mu \approx -\frac{1}{2}(I + A) \approx \frac{1}{2}(\epsilon_{\text{H}} + \epsilon_{\text{L}}) \quad (1)$$

and

$$\eta \approx \frac{1}{2}(I - A) \approx \frac{1}{2}(\epsilon_{\text{L}} - \epsilon_{\text{H}}), \quad (2)$$

where  $I$  is the first ionization potential and  $A$  the electron affinity of the neutral molecule, respectively. Koopman's theorem ( $I = -\epsilon_{\text{H}}$ ,  $A = -\epsilon_{\text{L}}$ ) allows one to write  $\mu$  and  $\eta$  in terms of the energies of the frontier highest occupied molecular orbital (HOMO,  $\epsilon_{\text{H}}$ ) and the lowest unoccupied molecular orbital (LUMO,  $\epsilon_{\text{L}}$ ) as indicated in the right-hand sides of Eqs. (1) and (2); this approach to  $\mu$  and  $\eta$  will be used here.

### 2.2 Transition state

In order to characterize the TS we will adopt a theoretical model described elsewhere [33–35], this model was successfully applied to the study of the keto  $\rightleftharpoons$  enol tautomerism [12]. Within this context, the TS is characterized by its position along the reduced reaction coordinate at  $\omega = \beta$ . Properties such as the energy barrier  $\Delta V^\ddagger = (V^\ddagger - V^\circ)$ , the activation chemical potential  $\Delta\mu^\ddagger = (\mu^\ddagger - \mu^\circ)$ , the activation hardness  $\Delta\eta^\ddagger = (\eta^\ddagger - \eta^\circ)$  and the activation polarizability  $\Delta\alpha^\ddagger = (\alpha^\ddagger - \alpha^\circ)$  are useful quantities to describe the properties of the TS structures with reference to the reactant species.

The Marcus equation [33–35, 44, 45] is also a useful tool to rationalize the energy of the TS. Within our model of a chemical reaction it takes the form

$$\Delta V^\ddagger = \left[ \frac{1}{4}K_{\text{V}} + \frac{1}{2}\Delta V^\circ + \frac{(\Delta V^\circ)^2}{4K_{\text{V}}} \right], \quad (3)$$

where  $K_{\text{V}}$  is an intrinsic property of the reaction (it is found to be the sum of the individual force constants associated with the potential wells describing reactants and products [33–35]) and  $\Delta V^\circ = [V(P) - V(R)]$  is the reaction energy, the energetic difference between product and reactant molecules.

The position of the TS along the reaction coordinate,  $\omega$ , is related to the activation energy through Leffler's definition of the Brønsted coefficient ( $\beta$ ) [46]:

$$\beta \equiv \frac{\partial \Delta V^\ddagger}{\partial \Delta V^\circ} \Rightarrow \beta = \frac{1}{2} + \frac{\Delta V^\circ}{2K_{\text{V}}}. \quad (4)$$

Since the TS is located at  $\omega = \beta$ , the  $\beta$  parameter measures the degree of resemblance of the TS to one of the R or P ground states. It is interesting to note that  $\beta$  provides a quantitative basis to discuss the Hammond postulate [43]: if  $\Delta V^\circ > 0$  then  $\beta > \frac{1}{2}$ , and the TS will be closer to the products, whereas if  $\Delta V^\circ < 0$  then  $\beta < \frac{1}{2}$ , the transition will be closer to the reactants.

Assuming that the TS results from interpolation of two harmonic potentials associated with reactants and products with individual force constants  $k_R$  and  $k_P$ , such that  $k_R + k_P = K_V$  [35], it can be shown that the curvature of the resulting potential-energy function at the TS,  $k(\beta)$ , is related to  $K_V$ ,  $\beta$  and  $\Delta V^\circ$  through the following equation [35]:

$$k(\beta) = -\frac{1}{2}K_V + \left(\beta - \frac{1}{2}\right)\Delta V^\circ . \quad (5)$$

Note that for symmetric (isoenergetic) reactions ( $\beta = 1/2$  and  $\Delta V^\circ = 0$ )  $k(\beta)$  becomes equal to the negative of the average of the force constants associated with the reactant and product potential wells. The energy barrier can now be expressed in terms of  $k(\beta)$ , leading to

$$\Delta V^\ddagger = -\frac{1}{2}k(\beta) + \beta\Delta V^\circ . \quad (6)$$

It is clear that  $k(\beta)$  can be seen as a negative force constant that should be related to the actual force constant associated with the imaginary frequency ( $k_{im}$ ) that defines the TS structure linking the two minima. If we assume  $k(\beta) \approx \lambda k_{im}$ , with  $\lambda$  a proportionality constant, we obtain a new energy barrier, now in terms of the force constant of the vibrational mode presenting the imaginary frequency

$$\Delta V_0^\ddagger = -\frac{1}{2}\lambda k_{im} + \beta\Delta V^\circ . \quad (7)$$

Comparison of numerical values of  $\Delta V_0^\ddagger$  with the optimized  $\Delta V^\ddagger$  values will determine if one can safely assume a simple linear relation between  $k(\beta)$  and  $k_{im}$ . It is important to stress the fact that Eq. (7) contains quantities associated with the three relevant states along the reaction coordinate: reactants, products and the TS.

### 3 Computational methods

Geometry optimization for the series of imines  $\text{CH}_3\text{CX}=\text{NH}$ , enamines  $\text{CH}_2=\text{CXNH}_2$  [ $X = \text{H, F, Cl, Br, NH}_2, \text{CH}_3, \text{OH}$  and  $\text{N}(\text{CH}_3)_2$ ] and the corresponding TS structures were performed at Hartree-Fock (HF), HF/6-311G\*\* and DFT/6-311G\*\* levels of theory using the Gaussian94 package [47]. The exchange-correlation functionals in all DFT calculations were taken to be Becke's three parameter functional including the gradient corrected correlation functional of Lee, Yang and Parr [48–50]. The molecular structures along the IRC were fully optimized at the same level of theory. The profiles of  $V$ ,  $\mu$ ,  $\eta$  and  $\alpha$  were obtained through single-point calculations of the fully optimized structures indicated by the IRC procedure. The chemical potential and hardness were calculated using Eqs. (1) and (2), respectively.

## 4 Results and discussion

### 4.1 Relative stability and MHP and MPP rules

Figure 1 schematically shows the three main structures involved in the tautomeric equilibria, including atom numbering. The values for the reaction energy  $\Delta V^\circ = V(\text{enamine}) - V(\text{imine})$  and the associated variations of  $\eta$  and  $\alpha$  are displayed in Table 1. It may be seen

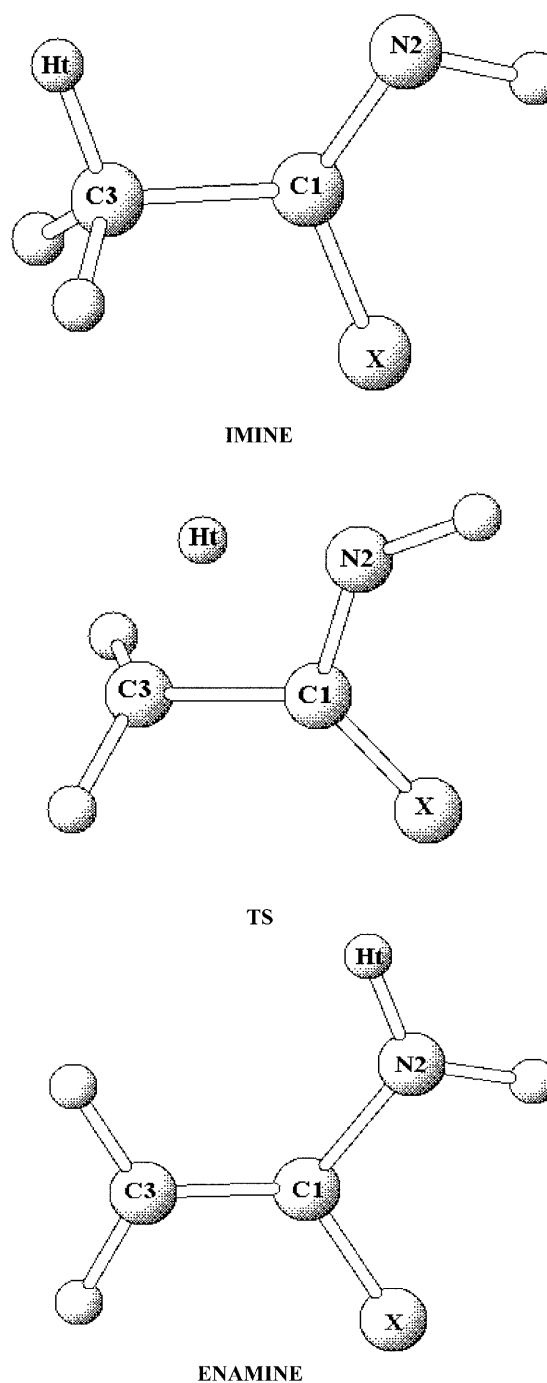


**Fig. 1.** Representation of the imine, transition state (TS) and enamine structures involved in the  $\text{CH}_3\text{CXNH} = \text{CH}_2\text{CXNH}_2$  interconversion

**Table 1.** Reaction and activation properties (energy, chemical potential, hardness and polarizability) for the  $\text{CH}_3\text{CX}=\text{NH} \rightleftharpoons \text{CH}_2=\text{CXNH}_2$  interconversion. The first entry corresponds to HF/6-311G\*\* calculations and the second entry corresponds to B3LYP/6-311G\*\* calculations. Energies and hardness are given in kilocalories per mole; polarizabilities are given in atomic units

$X$	$\Delta V^\circ$	$\Delta\eta^\circ$	$\Delta\alpha^\circ$	$\Delta V^\ddagger$	$\Delta\eta^\ddagger$	$\Delta\alpha^\ddagger$
H	6.1	-34.7	0.635	83.9	-41.4	3.747
	3.7	-7.9	0.059	66.9	-25.5	4.290
F	14.3	-41.6	0.981	88.2	-40.2	3.595
	13.1	-19.0	0.574	72.2	-31.7	4.311
Cl	12.6	-34.7	0.825	87.6	-44.1	3.993
	12.1	-13.7	0.531	71.3	-27.5	4.848
Br	12.7	-25.3	0.872	87.5	-33.1	4.117
	12.7	-18.1	1.344	71.4	-23.5	5.633
$\text{CH}_3$	5.3	-27.5	1.198	81.5	-36.1	3.501
	3.9	-8.2	1.060	65.5	-25.2	4.396
OH	10.9	-27.9	0.669	79.3	-30.5	3.402
	10.6	-22.3	0.016	65.0	-27.4	4.302
$\text{NH}_2$	9.4	-16.9	1.254	76.2	-26.5	3.425
	8.8	-10.7	1.241	61.8	-18.5	4.576
$\text{N}(\text{CH}_3)_2$	8.4	-9.9	2.080	72.3	-19.6	4.089
	8.1	-11.4	1.897	58.2	-18.0	5.918

that in all cases the imine tautomers have lower energy than their enamine counterparts, in agreement with previous results [21, 22]. We also note that in all the cases presented here  $\Delta\eta^\circ < 0$ , indicating that the substituted imines are harder than the enamine species. From the  $\Delta V^\circ$  and  $\Delta\eta^\circ$  values we find that the relative order of stability in each imine–enamine pair coincides with variations in chemical hardness that are consistent with the MHP. On the other hand, positive values of  $\Delta V^\circ$  are correlated with positive values of  $\Delta\alpha^\circ$  for each imine–enamine pair, in agreement with the MPP. Activation energies  $\Delta V^\ddagger = V^\ddagger - V(\text{imine})$ , activation hardnesses  $\Delta\eta^\ddagger = \eta^\ddagger - \eta(\text{imine})$  and activation polarizabilities  $\Delta\alpha^\ddagger = \alpha^\ddagger - \alpha(\text{imine})$  are also quoted in Table 1. It may be seen that  $\Delta V^\ddagger$  is associated with negative variations in chemical hardness, showing that for each molecule an MHP-like relationship holds: the TS for each structure considered is consistently softer than the corresponding imine ground state. Also, positive variations of  $\Delta V^\ddagger$  are associated with positive variations of polarizability: the TS structure is the most polarizable species, in agreement with the MPP rule.

To validate these results we determined  $\Delta V^\circ$  and  $\Delta V^\ddagger$  using DFT calculations at the B3LYP/6-311G\*\* level of theory. Even though these calculations roughly present the same variation pattern for  $\Delta V^\circ$  and  $\Delta V^\ddagger$  as the HF/6-311G\*\* level, we have found that the electronic properties do not follow the expected trends; this is probably due to the systematic presence of bound LUMO states in the reference structures. The major effect of having bound LUMOs is reflected in the fact that the chemical hardness will be determined from the difference of the absolute values of  $\varepsilon_L$  and  $\varepsilon_H$  and, therefore,  $\eta$  will appear to be underestimated, as is shown in the second entry of Table 1.

A better appraisal of the results, combining the variations in  $V$ ,  $\eta$ ,  $\mu$  and  $\alpha$ , may be achieved by looking at the profiles displayed in Fig. 2. The imine forms are located at the negative region of the IRC (at  $\omega = 0$ ). In all cases, the energy profile presents a quite sharp maximum representing the TS.  $\Delta\mu$ ,  $\Delta\eta$  and  $\Delta\alpha$  values also present a critical point at or very near the TS. One of the most relevant features of Fig. 2 is that  $\Delta\eta$  presents opposite behavior with respect to the energy profile, confirming the validity of the MHP along the reaction coordinate for the intramolecular proton transfer. We also observe that the variations of the chemical potential along the IRC or  $\omega$  coordinate are intermediate between the variations of  $V$  and  $\eta$ ; this has been observed previously in different systems [12, 34, 51]. On the other hand, the polarizability displays a profile similar to that of the energy; in all cases  $\Delta\alpha$  is a minimum for the most stable structure. The inverse behavior of the profiles of  $\alpha$  and  $\eta$  shows the simultaneous validity of the MHP and the MPP along the reaction coordinate.

It is well known that the polarizability is better represented using a Sadlej basis set [52] although it was recently shown [53] that the use of a Pople basis set leads to the same qualitative trend. The polarizability profiles for the systems substituted with  $X = \text{F}$ , Cl and Br, using the Pople basis set, are shown in Fig. 3. It may be seen that the increasing order  $\alpha(\text{F}) < \alpha(\text{Cl}) < \alpha(\text{Br})$  along the reaction coordinate is the same as for the global softness (S) [23, 24]. For instance, for the imine ground state the global softness order is  $\text{F}(S = 3.32 \text{ au}) < \text{Cl}(S = 3.43 \text{ au}) < \text{Br}(S = 3.69 \text{ au})$ . At the TS the corresponding order is  $\text{F}(S = 4.22 \text{ au}) < \text{Cl}(S = 4.51 \text{ au}) < \text{Br}(S = 4.58 \text{ au})$ . Note that at the TS the maximum value of the polarizability coincides with the maximum value of the softness, because the enamine ground states display softness values that are between those of the imine ground states and TS:  $\text{F}(S = 4.15 \text{ au}) < \text{Cl}(S = 4.23 \text{ au}) < \text{Br}(S = 4.33 \text{ au})$ .

#### 4.2 Brønsted coefficients and Hammond postulate

Besides the MHP and MPP rules, the Marcus equation allows one to rationalize the energy barrier for the intramolecular proton transfer. All the parameters allowing the characterization of the TS structures at both HF and B3LYP levels of theory are collected in Table 2. From the optimized  $\Delta V^\ddagger$  and  $\Delta V^\circ$  values we have determined  $K_V$  through Eq. (3); the Brønsted coefficients  $\beta$  are then obtained from Eq. (4). It may be seen that for the whole series the  $\beta$  values are very close to 1/2, indicating that at the TS the transferred proton is about midway between the corresponding donor and acceptor atoms. This behavior is typical in reactions with large activation energies [54], as in the present case. The use of linear free-energy relationships, such as the Hammett equation [55], or the use of the slopes of structure–reactivity correlations, specifically the Brønsted coefficients to characterize TS structures [56, 57], has come under criticism in recent years [58]. However the above result shows that a qualitative discussion of the TS in terms of the Marcus equation and Brønsted coefficients is possible.

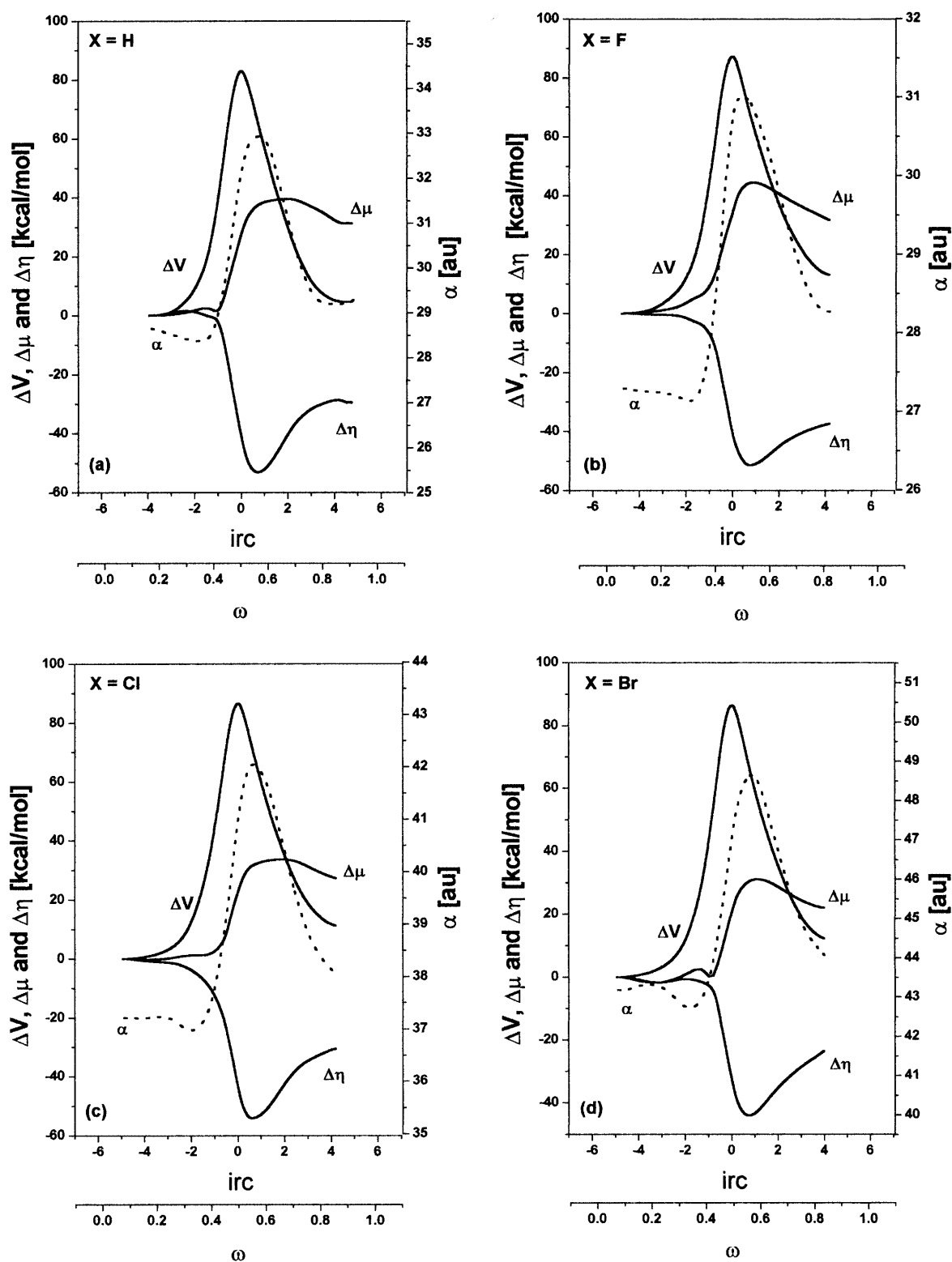


Fig. 2. Potential energy electronic chemical potential, hardness and polarizability profiles at the HF/6-31G\*\* level for the  $\text{CH}_3\text{CXNH} = \text{CH}_2\text{CXNH}_2$  interconversion

Columns four and five of Table 2 display the values of  $k(\beta)$  obtained from Eq. (5) and  $k_{\text{im}}$  obtained from standard frequency calculations. Both quantities are related through the parameter  $\lambda$ , shown in the sixth col-

umn of Table 2. We note that  $\lambda$  is quite constant along the series, with average values of 0.353 and 0.354 for the HF and B3LYP calculations, respectively. With this value at hand, we calculated the energy barriers  $\Delta V_0^\ddagger$

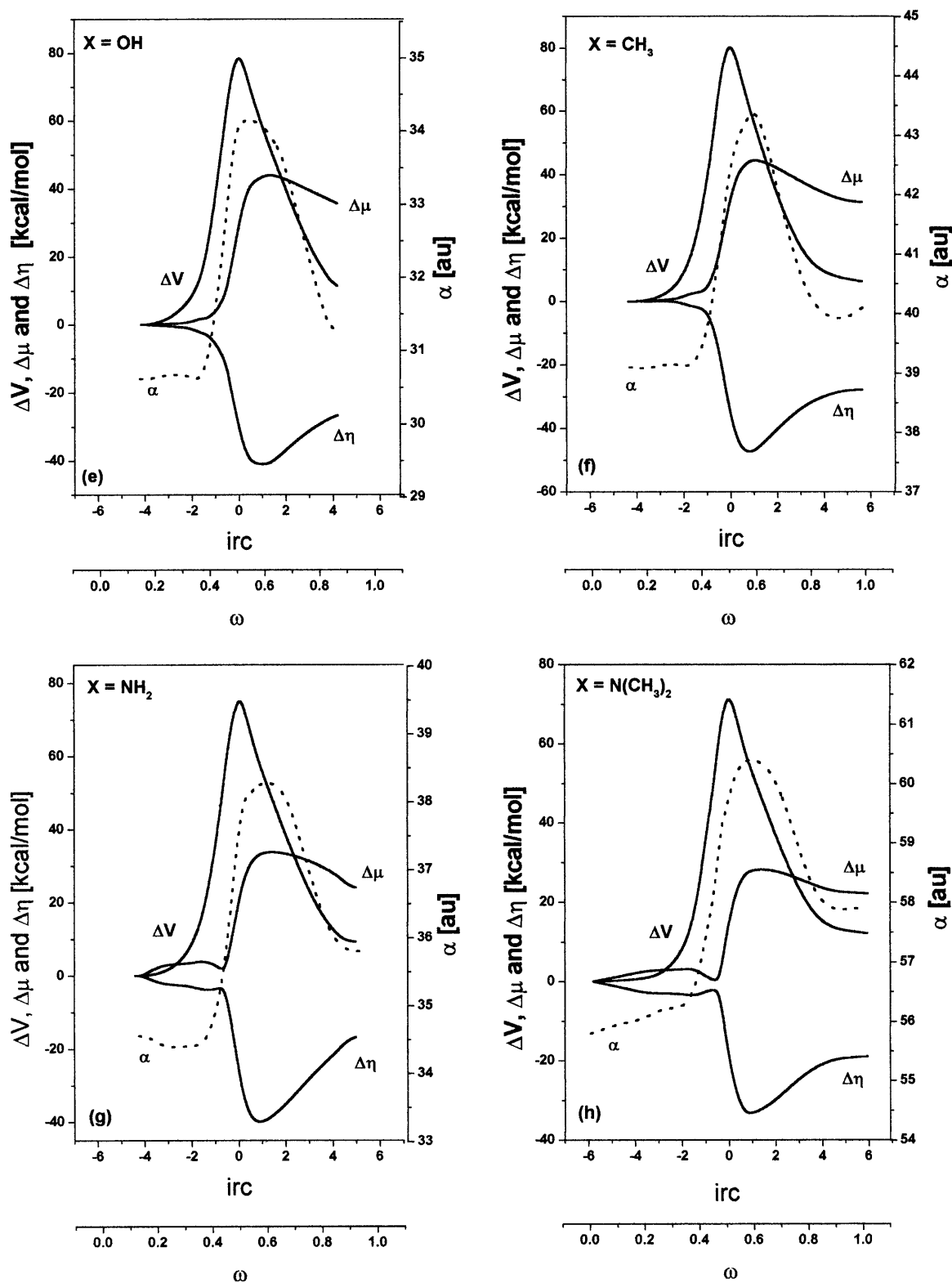


Fig. 2. (Contd)

from Eq. (7); the results are very close to the optimized values ( $\Delta V^\ddagger$ ). The relative errors indicated in the last column of Table 2 are less than 4%; this indicates that in this series of molecules our assumption about linear

proportionality between  $k(\beta)$  and  $k_{\text{im}}$  applies. On the other hand, it is important to mention that the consistency reached between  $k(\beta)$  and  $k_{\text{im}}$  validates the models we used to analyze our results.

## 4.3 Substituent effects

In order to study the effect of chemical substitution on the activation parameters we define relative quantities with reference to the unsubstituted molecule ( $X = \text{H}$ ) as follows:

$$\delta\Delta P^\ddagger = \Delta P^\ddagger(X) - \Delta P^\ddagger(\text{H}) , \quad (8)$$

for any property  $P$ . Equation (8) quantifies the effect of chemical substitution on the activation property and may be further developed to determine the effect of chemical substitution on both the TS structures and the reference ground states. Using the definitions  $\Delta P^\ddagger(X) =$

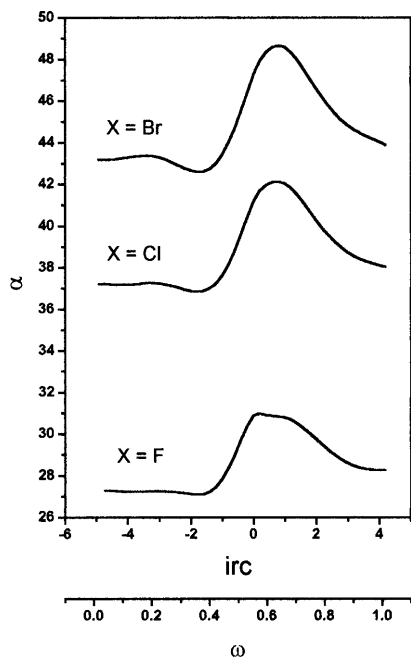


Fig. 3. HF/6-311G\*\* polarizability profiles for the halogen imines

**Table 2.** Transition-state parameters for  $\text{CH}_3\text{CX} = \text{NH} \rightleftharpoons \text{CH}_2 = \text{CXNH}_2$  equilibria. All values are in kilocalories per mole. The first entry corresponds to HF/6-311G\*\* calculations and the second entry corresponds to B3LYP/6-311G\*\* calculations

$X$	$K_V$	$\beta$	$k(\beta)$	$k_{\text{im}}$	$\lambda$	$\Delta V^\ddagger$	$\Delta V_0^\ddagger$	% error
H	323.5	0.5094	-161.7	-445.5	0.363	83.9	81.7	2.6
	260.2	0.5072	-130.1	-360.7	0.361	66.9	65.7	1.8
F	324.1	0.5218	-161.8	-461.6	0.350	88.2	88.9	0.8
	261.9	0.5250	-130.6	-363.6	0.359	72.2	71.2	1.4
Cl	324.8	0.5194	-162.2	-479.2	0.338	87.6	91.1	4.0
	260.1	0.5234	-129.8	-376.4	0.345	71.3	73.0	2.4
Br	323.9	0.5196	-161.7	-477.2	0.339	87.5	90.8	3.8
	259.4	0.5245	-129.4	-378.3	0.342	71.4	73.6	3.1
$\text{CH}_3$	315.5	0.5084	-157.1	-433.7	0.364	81.5	79.2	2.8
	254.3	0.5077	-127.1	-354.0	0.359	65.5	64.6	1.5
OH	294.7	0.5186	-147.2	-415.3	0.354	79.3	79.0	0.4
	238.4	0.5222	-118.9	-333.9	0.356	65.0	64.6	0.6
$\text{NH}_2$	285.8	0.5164	-142.7	-403.2	0.354	76.2	76.0	0.3
	229.4	0.5192	-114.5	-319.6	0.358	61.8	61.1	1.1
$\text{N}(\text{CH}_3)_2$	272.4	0.5154	-136.0	-399.5	0.341	72.3	74.8	3.5
	216.0	0.5188	-107.9	-309.3	0.349	58.2	58.9	1.2

$P^\ddagger(X) - P^\circ(X)$  and  $\Delta P^\ddagger(\text{H}) = P^\ddagger(\text{H}) - P^\circ(\text{H})$ , we obtain from Eq. (8):

$$\begin{aligned} \delta\Delta P^\ddagger &= [P^\ddagger(X) - P^\ddagger(\text{H})] - [P^\circ(X) - P^\circ(\text{H})] \\ &= (\Delta_s P^\ddagger - \Delta_s P^\circ) . \end{aligned} \quad (9)$$

The first term of Eq. (9) contains the effect of chemical substitution on the property  $P$  at the TS, whereas the second contribution represents the effect of the substituent on the reactant state (imine form in this case). When  $\delta\Delta P^\ddagger > 0$ , we find that  $\Delta_s P^\ddagger > \Delta_s P^\circ$  and the effect due to the substituent is larger on the TS than on the reactant species. In contrast to this, when  $\delta\Delta P^\ddagger < 0$ , we find that  $\Delta_s P^\ddagger < \Delta_s P^\circ$ ; in this case the effect due to the substituent is larger on the reactant than on the TS.

The variations of the energy barrier with respect to the reference system are characterized through  $\delta\Delta V^\ddagger$  and numerical values at the HF/6-311G\*\* level of calculation are displayed in the second column of Table 3. We note that  $\delta\Delta V^\ddagger > 0$  is obtained for the systems with F, Cl and Br, usually classified as electron-withdrawing chemical groups. In these cases  $\Delta_s V^\ddagger > \Delta_s V^\circ$  and the electron-withdrawing character for these substituents acts mainly on the TS structure, destabilizing it with the result of an increase in the activation energy with respect to the reference system. On the other hand, systems with  $X = \text{CH}_3$ , OH,  $\text{NH}_2$  and  $\text{N}(\text{CH}_3)_2$  groups, which are classified as electron donors, present  $\delta\Delta V^\ddagger < 0$ ; this implies that  $\Delta_s V^\ddagger < \Delta_s V^\circ$ . These groups mainly act on the stable imine reference species, resulting in a decrease in the activation barrier with respect to the reference system.

In the case of activation hardness we found that in all cases with the only exception of  $X = \text{Cl}$ ,  $\delta\Delta\eta^\ddagger > 0$ , indicating that  $\Delta\eta^\ddagger(X) > \Delta\eta^\ddagger(\text{H})$ . Since  $\Delta\eta^\ddagger(i)$  is negative for any species  $i = X, \text{H}$  then  $|\Delta\eta^\ddagger(X)| < |\Delta\eta^\ddagger(\text{H})|$  as can be verified from Table 1. From Eq. (9), this last outcome implies that  $\Delta_s\eta^\ddagger < \Delta_s\eta^\circ$ , and so the variations in chemical hardness at the ground states promoted by the substituent effects become more significant than the

**Table 3.** Variations of activation parameters for  $\text{CH}_3\text{CX}=\text{NH} \rightleftharpoons \text{CH}_2=\text{CXNH}_2$  interconversion at the HF/6-311G\*\* level of theory. Energy and hardness values are in kilocalories per mole; polarizabilities values are in atomic units

$X$	$\delta\Delta V^\ddagger$	$\delta\Delta\eta^\ddagger$	$\Delta_s\eta^\ddagger$	$\Delta_s\eta^\circ$	$\delta\Delta\alpha^\ddagger$	$\Delta_s\alpha^\ddagger$	$\Delta_s\alpha^\circ$
H	0.0	0.0	0.0	0.0	0.0	0.0	0.0
F	4.3	1.2	11.2	10.0	-0.15	-1.50	-1.35
Cl	3.7	-2.7	1.4	4.1	0.25	8.80	8.55
Br	3.5	8.3	-0.5	-8.8	0.37	14.89	14.52
$\text{CH}_3$	-2.4	5.3	-1.0	-6.3	-0.25	10.20	10.45
OH	-4.7	10.9	1.0	-9.9	-0.34	1.62	1.96
$\text{NH}_2$	-7.7	14.9	-4.2	-19.1	-0.32	5.59	5.91
$\text{N}(\text{CH}_3)_2$	-11.6	21.8	-4.2	-26.0	0.34	27.49	27.15

ones observed at the TS structures, as is shown in Table 3. On the other hand, since  $\eta^\ddagger(X)$  is always positive, positive values of  $\Delta_s\eta^\ddagger$  indicate that the TS for the  $X$ -substituted system is harder than the TS of the reference system. Similarly, positive values of  $\Delta_s\eta^\circ$  indicate that the  $X$ -substituted imine is harder than the corresponding reference system. Conversely, negative values of  $\Delta_s\eta^\ddagger$  and  $\Delta_s\eta^\circ$  indicate that the unsubstituted species are harder than the substituted ones. It is interesting to note in Table 3 that in most cases  $\Delta_s\eta^\ddagger$  and  $\Delta_s\eta^\circ$  have the same sign, indicating that the effect of the substituent is in the same sense for TSs and reference imine forms. For the variations in the activation polarizability we found that  $\Delta_s\alpha^\ddagger$  and  $\Delta_s\alpha^\circ$  have the same sign and order of magnitude. In general, we observe a similar effect of chemical substitution on both the TSs and the reference imine forms.

## 5 Summary and concluding remarks

A global analysis on the imine  $\rightleftharpoons$  enamine tautomerism for a series of eight imine derivatives  $\text{CH}_3\text{CXNH}$  has been performed. In all cases the imine tautomers are more stable than the enamine ones. The relative stability between reactants, TSs and products follows order relationships that are consistent with the MHP and the MPP.

We have rationalized the imine–enamine tautomerism by combining DFT concepts with properties such as force constants and energy barriers. The Marcus equation has been used to rationalize the energy barriers for intramolecular proton transfer and accurate values of them may be obtained through an empirical formula involving the force constant of the mode presenting the imaginary frequency of the TS.

Substituent effects on the barrier to intramolecular proton transfer manifest themselves through differential inductive effects: while the electron donor groups stabilize the TS structure, the electron-withdrawing groups ( $X = \text{F}, \text{Cl}$  and  $\text{Br}$ ) increase the energy barrier with reference to the unsubstituted system ( $X = \text{H}$ ). Substituent effects may be also analyzed in a partitioned form to probe the effect of the substituent group at the ground state and the TS structures in terms of the variations of the activation hardness and polarizability with respect to the system with  $X = \text{H}$ .

*Acknowledgements.* This work was supported by FONDECYT through project nos. 3990033 and 1990543 and by the Cátedra Presidencial en Ciencias awarded to A.T.L.

## References

- Rappoport Z (ed) (1990) The chemistry of enols. Wiley, Chichester
- Capon B, Guo B-Z, Kowk FK, Siddhanta AK, Zucco C (1988) *Acc Chem Res* 21: 135
- Rappoport Z, Biali SE (1988) *Acc Chem Res* 21: 442
- Kwiatkowski JS, Zielinski TJ, Rein R (1986) *Adv Quantum Chem* 18: 85
- Hart H (1979) *Chem Rev* 79: 515
- Lovas FJ, Clark FO, Tiemann E (1975) *J Chem Phys* 62: 1925
- Keefe JR, Kresge AJ, Schepp NP (1990) *J Am Chem Soc* 112: 4862
- Keefe JR, Kresge AJ, Schepp NP (1988) *J Am Chem Soc* 110: 1993
- Saunders WH (1994) *J Am Chem Soc* 116: 5400
- Bernasconi CF, Wenzel PJ (1994) *J Am Chem Soc* 116: 5405
- Andrés J, Domingo LR, Picher MT, Safont VS (1998) *Int J Quantum Chem* 66: 9
- Pérez P, Toro-Labbé A (2000) *J Phys Chem A* 104: 1557
- Leermaker JA (1933) *J Am Chem Soc* 55: 3098
- Rice FO, Grelecki CT (1957) *J Phys Chem* 61: 830
- Collin JE, Franskin MJ (1966) *Bull Soc R Sci Liege* 35: 267
- Johnson DR, Lovas FJ (1972) *Chem Phys Lett* 65: 1925
- Gordon MS, Pople JA (1968) *J Chem Phys* 49: 4643
- Moffat JB (1970) *Can J Chem* 48: 1820
- Lovas FJ, Suenram RD, Johnson DR (1980) *J Chem Phys* 72: 4964
- Pross A, Radom L, Riggs NV (1980) *J Am Chem Soc* 71: 2253
- Lammertsma K, Prasad BV (1994) *J Am Chem Soc* 116: 642
- Lin J-F, Wu C-C, Lien M-H (1995) *J Phys Chem* 99: 16903
- Parr RG, Yang W (1989) *Density functional theory of atoms and molecules*. Oxford University Press, New York
- Pearson RG (1997) *Chemical hardness*. Wiley-VCH, New York
- Dreizler RM, da Providencia J (1975) *Density functional methods in physics*. Plenum, New York
- Parr RG, Donnelly RA, Palke WE (1978) *J Chem Phys* 68: 3801
- Parr RG, Pearson RG (1983) *J Am Chem Soc* 105: 7512
- Pearson RG (1985) *J Am Chem Soc* 107: 6801
- Yang W, Parr RG (1985) *Proc Natl Acad Sci* 82: 6723
- (a) Parr RG, Yang W (1984) *J Am Chem Soc* 106: 4049; (b) Yang W, Parr RG, Pucci R (1984) *J Chem Phys* 81: 2862
- (a) Kar T, Scheiner S, Sannigrahi AB (1998) *J Phys Chem A* 102: 5967; (b) Arulmozhiraja S, Kolandaivel P (1997) *Int J Quantum Chem* 64: 231; (c) Kar T, Scheiner S (1995) *J Phys Chem* 99: 8121; (d) Mineva T, Sicilia E, Russo N (1998) *J Am Chem Soc* 120: 9053; (e) De Proft F, Amira S, Choho K, Geerlings P (1994) *J Phys Chem* 98: 5227; (f) Safi B, Choho F, De Proft F, Geerlings P (1998) *J Phys Chem A* 102: 5253; (g) Méndez F, Gázquez JL (1994) *J Am Chem Soc* 116: 9298; (h) Bird CW (1997) *Tetrahedron* 53: 3319; (i) Kaschner R, Hohl D (1998) *J Phys Chem A* 102: 5111; (j) Baeten A, De Proft F, Geerlings P (1996) *Int J Quantum Chem* 60: 931
- (a) Chattaraj PK, Nath S, Sannigrahi AB (1993) *Chem Phys Lett* 212: 223; (b) Chattaraj PK, Nath S, Sannigrahi AB (1994) *J Phys Chem* 98: 9143; (c) Nath S, Sannigrahi AB, Chattaraj PK (1994) *J Mol Struct (THEOCHEM)* 309: 65
- (a) Cárdenas-Jirón GI, Lahsen J, Toro-Labbé A (1995) *J Phys Chem* 99: 5325; (b) Cárdenas-Jirón GI, Toro-Labbé A (1995) *J Phys Chem* 99: 12730; (c) Cárdenas-Jirón GI, Gutiérrez-Oliva S, Melin J, Toro-Labbé A (1997) *J Phys Chem A* 101: 4621
- Toro-Labbé A (1999) *J Phys Chem A* 103: 4398
- Gutiérrez-Oliva S, Letelier JR, Toro-Labbé A (1999) *Mol Phys* 96: 61
- Pearson RG (1987) *J Chem Educ* 64: 561
- Parr RG, Chattaraj PK (1991) *J Am Chem Soc* 113: 1854



38. (a) Chattaraj PK, Lee H, Parr RG (1991) *J Am Chem Soc* 113: 1855; (b) Chattaraj PK, Schleyer PvR (1994) *J Am Chem Soc* 116: 1067
39. (a) Politzer P (1987) *J Chem Phys* 86: 1072; (b) Fuentealba P, Reyes O (1993) *J Mol Struct (THEOCHEM)* 282: 65; (c) Ghanty TK, Ghosh SK (1993) *J Phys Chem* 97: 4951
40. Chattaraj PK, Sengupta SJ (1996) *J Phys Chem* 100: 16126
41. (a) Chattaraj PK, Poddar A (1998) *J Phys Chem A* 102: 9944; (b) Chattaraj PK, Poddar A (1999) *J Phys Chem A* 103: 1274
42. Gutiérrez-Oliva S, Jaque P, Toro-Labbé A (2000) *J Phys Chem A* 104: 8955
43. Hammond GS (1955) *J Am Chem Soc* 77: 334
44. Sola M, Toro-Labbé A (1999) *J Phys Chem A* 103: 8847
45. Marcus RA (1964) *Annu Rev Phys Chem* 15: 155
46. Leffler JE (1953) *Science* 117: 340
47. Frisch MJ, Trucks GW, Schlegel HB, Gill PMW, Johnson BG, Robb MA, Cheeseman JR, Keith TA, Peterson GA, Montgomery JA, Raghavachari K, Al-Laham MA, Zakrzewski VG, Ortiz JV, Foresman JB, Ciolowski J, Stefanov BB, Nanayakkara A, Challacombe M, Peng CY, Ayala PY, Chen W, Wong MW, Andres JL, Replogle ES, Gomperts R, Martin RL, Fox DJ, Binkley JS, Defrees DJ, Baker J, Stewart JP, Head-Gordon M, González C and Pople JA (1995) *Gaussian 94*, Gaussian Pittsburgh, PA
48. Lee C, Yang W, Parr RG (1988) *Phys Rev B* 37: 785
49. Miehlich B, Savin A, Stoll H, Preuss H (1989) *Chem Phys Lett* 157: 200
50. Becke AD (1993) *J Chem Phys* 98: 5648
51. Jaque P, Toro-Labbé A (2000) *J Phys Chem A* 104: 995
52. (a) Sadlej AJ (1988) *Collect Czech Chem Commun* 53: 1995; (b) Sadlej AJ, Urban M (1991) *J Mol Struct (THEOCHEM)* 234: 147
53. Chattaraj PK, Fuentealba P, Jaque P, Toro-Labbé A (1999) *J Phys Chem A* 103: 9307
54. Petersson GA, Tensfeldt TG, Montgomery JA Jr (1992) *J Am Chem Soc* 114: 6133
55. (a) Hammett LP (1937) *J Am Chem Soc* 59: 96; (b) Pérez P, Simón-Manso Y, Aizman A, Fuentealba P, Contreras R (2000) *J Am Chem Soc* 122: 4756
56. Williams IH, Austin PA (1999) *Can J Chem* 77: 830
57. Williams IH (1988) *Bull Soc Chim Fr* 192
58. Pross A, Shaik S (1989) *Nouv J Chim* 13: 427